INTEGRATED HE-LHC OPTICS AND ITS PERFORMANCE*

M. Hofer[†1], M. Crouch, J. Keintzel[1], T. Risselada, R. Tomás, F. Zimmermann
CERN, Geneva, Switzerland
D. Zhou, KEK, Tsukuba, Japan
L. van Riesen-Haupt, John Adams Institute, University of Oxford, UK
Y. Nosochkov, SLAC, Stanford, USA
[1]also at Vienna University of Technology, Vienna, Austria

Abstract

One possible future hadron collider design investigated in the framework of the Future Circular Collider (FCC) study is the High-Energy LHC (HE-LHC). Using the 16 T dipoles developed for the FCC-hh the center of mass energy of the LHC is set to increase to 27 TeV. To achieve this set energy goal, a new optics design is required, taking into account the constraint from the LHC tunnel geometry. In this paper, two different lattices for the HE-LHC are presented. Initial considerations take into account the physical aperture at the proposed injection energy as well as the energy reach of these lattices. The dynamic aperture at the injection energies is determined using latest evaluations of the field quality of the main dipoles.

INTRODUCTION

As part of the Future Circular Collider study, the option to upgrade the Large Hadron Collider (LHC) is investigated. Using the 16 T dipoles presently under investigation for the FCC-hh, the target beam energy is set to increase to 13.5 TeV. This High Energy LHC (HE-LHC) will be housed in the same tunnel as the LHC and LEP before with no major civil engineering being required for the installation. The goal is to achieve an integrated luminosity of 10 ab^{-1} in about 20 years of operation in two high luminosity experiments. These will be housed in the same location as the current experiments ATLAS and CMS. The overall layout of HE-LHC remains as in the LHC with the injection of the beams taking place in IR2 and IR8, a momentum collimation section in IR3, a RF-insertion in IR4, IR6 being the beam dump insertion for both beams, and a betatron collimation section in IR7. The same injected beam parameters as for High Luminosity LHC are foreseen for the HE-LHC (see Table 1). As an injector for the HE-LHC the current Super Proton Synchrotron (SPS) is considered with an injection energy of 450 GeV. In addition, the option of upgrading the SPS is also studied, which would allow for a higher injected beam energy of up to 1300 GeV.

LATTICES

For the HE-LHC, two different lattices are currently being looked into. The first one consists of 18 FODO cells per arc with a phase advance of 90 degree. To reach the center

Table 1: Comparison between (HL-)LHC and HE-LHC Parameters [1–3]

Parameter		(HL-) LHC	HE-LHC
Center of mass energy	[TeV]	14	27
Circumference	[km]	26.658	26.658
Dipole Field	[T]	8.3	16
Norm. Emittance	[µm]	(2.5) 3.75	2.5
Peak Luminosity per IP	[10^{34}cm^{-2}s^{-1}]	(12.6) 1	28
$\beta^*_{x,y}$	[µm]	(0.15) 0.55	0.25
No. of bunches per beam		2760	2808
Bunch Population	[10^{11}]	(2.2) 1.15	2.2
Beam Current	[A]	(1.1) 0.58	1.12
Bunch Spacing	[ns]	25	25

of mass collision energy of 27 TeV a higher dipole filling factor than the LHC is required, which is the case for this layout. Other layouts with 24 arc cells and 20 arc cells were also looked into and a detailed comparison is presented in [4]. This layout also provides some margin with the dipole field, allowing to shorten the dipoles and use this space for placing, for example, additional corrector elements should later studies conclude those are needed. The second option under study is a LHC-like lattice with 23 FODO cells per arc and a phase advance of 90 degree per cell. The cell layout had to be slightly modified to comply with the specified inter magnet distances for Nb$_3$Sn magnets. In order to fulfill those, the dipoles in this 23 arc cells layout had to be shortened, which together with the lower filling factor limits the energy reach. The arc cell parameters for both lattice options are presented in Table 2 and the layouts are presented in Fig. 1.

Table 2: Arc Cell Parameters for the Two Studied HE-LHC Lattices

Parameter		18 Cells	23 Cells
Cell length	[m]	137.227	106.9
Cell Phase advance	[°]	90	90
Number of dipoles per Cell		8	6
Dipole Length	[m]	13.95	13.83
Quadrupole Length	[m]	2.8	3.5
Sextupole Length	[m]	0.5	0.836
Dipole field for 13.5 TeV	[T]	15.83	16.59
Beam energy at 16 T	[TeV]	13.64	13.005

(a) Arc half-cell in the 18 cells layout

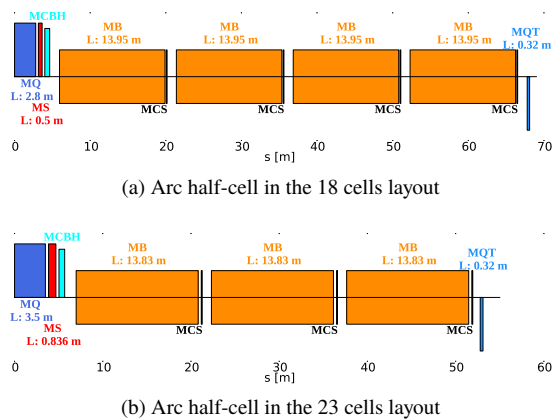(b) Arc half-cell in the 23 cells layout

Figure 1: Comparison of the half-cells in both lattices.

Physical Aperture

Using the APERTURE module in MAD-X [5], the beam stay clear is determined for both arc cells with the aperture parameter specified in [6] and assuming a mechanical tolerance of 1 mm. For the beam screen, the model developed for the FCC-hh was used as the synchrotron radiation load will be similar to this accelerator [7]. For HL-LHC, the minimum aperture considered to be safe is 12.6 σ [6], which, assuming improved tolerances, could go down to around 10 σ for the HE-LHC [8]. However, detailed collimation studies taking into account various loss scenarios are still required to determine a precise target aperture. The beam stay clear for the three considered injection energies is presented in Fig. 2 for the both layouts.
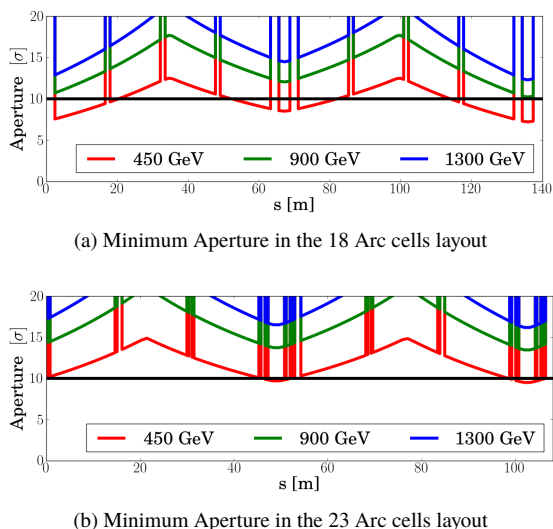

(a) Minimum Aperture in the 18 Arc cells layout

(b) Minimum Aperture in the 23 Arc cells layout

Figure 2: Comparison of the minimum aperture for different injection energies in both lattices. The target aperture of 10 σ is marked with a black line.

For the 18 arc cell layout, the minimum aperture is 7.3 σ at 450 GeV which is considerably below the above mentioned target aperture of 10 σ. The 23 Arc cell layout on the other hand provides an aperture of 9.5 σ, but is limited in

the collision energy to 26.01 TeV. In cases of an increased injection energy of 900 GeV and 1300 GeV the aperture in the 18 arc cells layout would increase to 10.3 σ and 12.3 σ, respectively.

Lattice Integration

For the full lattice, LHC-like dispersion suppressors were then used for both layouts which are illustrated in Fig. 3. For the high luminosity experiments, the layout presented

(a) Dispersion Suppressor in the 18 cells layout
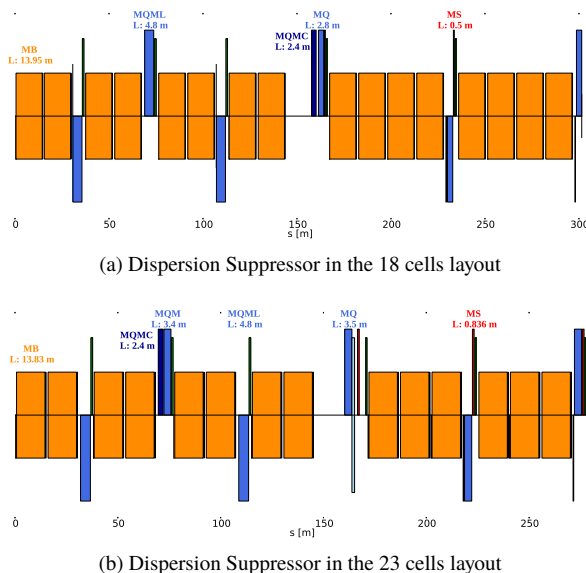

(b) Dispersion Suppressor in the 23 cells layout

Figure 3: Comparison of the dispersion suppressors in both lattices.

in [9] has been integrated. Currently, these insertions do not provide enough flexibility for the phase advance matching to allow for a good correction of the spurious dispersion caused by the crossing angle. A new layout for the RF-insertion in IR4 has been integrated [10]. Compared to the LHC, it features two more matching quadrupoles with more flexibility for matching the phase advance over the insertion. This insertion is then also used to adjust the tune of the whole ring. For the remaining insertions the layouts of the LHC were used and matched to the constraints from the two arc layouts. The tunes of the rings are then matched by adjusting the phase advance in the FODO cells in the Arcs 23, 34, 67, and 78. A phase advance of $\pi/2$ is kept in the arc cells adjacent to the experimental insertion to ensure an efficient correction of the chromaticity. Fine tuning is then achieved by changing the phase advance of the RF-insertion. As the lattice is constrained by the LEP tunnel geometry, the survey of the lattices is checked with the survey of LEP as a reference. The offset of both lattices to LEP is shown in Fig. 4. Taking into account the outer cryostat width and a safety margin to other elements the additional offset of 5 cm of the 18 arc cell lattice with respect to the LHC-like lattice needs to be checked with tunnel integration studies.

01 Circular and Linear Colliders
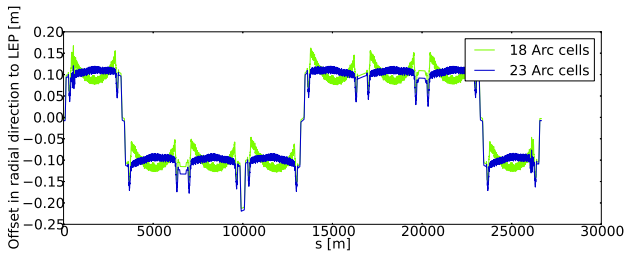
A01 Hadron Colliders

Figure 4: Transverse offset of both lattices with respect to LEP.

DYNAMIC APERTURE AT INJECTION ENERGY

The field quality of the main dipoles is one of the key factors for the beam stability at injection energy. To quantify the impact of magnetic imperfections on the beam, the dynamic aperture (DA) is evaluated with particle tracking simulations using the SixTrack code [11]. The multipole harmonics in the magnetic field expansion are described by [12]

$$b_n = b_{nS} + \frac{\xi_U}{1.5} b_{nU} + \xi_R b_{nR} \qquad (1)$$

where b_{nS}, b_{nU}, and b_{nR} are the systematic, uncertainty and random error component and ξ_U and ξ_R denote random numbers with a Gaussian distribution cut at $1.5\,\sigma$ and $3\,\sigma$, respectively. The same random number ξ_U is used for all dipoles in one arc whereas ξ_R is different for each dipole. The magnetic field error table presented in Table 3 was used. Note that here the field quality is presented for the inner aperture of the dipole and that even normal components change sign between the inner and outer aperture.

Table 3: Field Quality of the 16 T Dipoles for Various Injection Energies in Units of 10^{-4} at a Reference Radius of 16.7 mm. Note that currently the random and uncertainty component share the same values. The full error table including skew components can be found in [13].

Energy [GeV]	Systematic			Uncertainty		
	450	900	1300	450	900	1300
b_3	-35.0	-55.0	-40.0	10.0	4.00	3.00
b_4	0.0	0.0	0.0	0.449	0.449	0.449
b_5	8.0	8.0	4.0	1.500	1.500	0.800
b_6	0.0	0.0	0.0	0.176	0.176	0.176
b_7	0.2	0.6	1.1	0.211	0.211	0.211
b_8	0.0	0.0	0.0	0.071	0.071	0.071
b_9	3.8	4.2	2.9	0.500	0.500	0.200
b_{10}	0.0	0.0	0.0	0.027	0.027	0.027
b_{11}	0.75	0.86	1.00	0.028	0.028	0.028

The particles pairs are tracked for 10^5 turns in 60 different variations of the machine. For these DA studies five differ-

ent phase space angles and a relative momentum deviation of $7.5 \cdot 10^{-4}$ are used. This momentum deviation corresponds to 75% of the bucket height at an injection energy of 450 GeV. For higher injection energies the fraction of the bucket height depends amongst others on the injector design but the deviation is set to go down with increasing energy, making this assumption rather pessimistic. In the current correction scheme, the b_3-error of the dipoles is locally corrected with one spool piece corrector attached to each dipole with all correctors in one arc belonging to the same family. As in the LHC, in the 23 cell lattice every second dipole is equipped with a nested octupole and decapole spool piece for correcting b_4 and b_5 errors. In the 18 cell lattice 3 out of 8 dipoles per cell are equipped with such correctors. The number of these correctors is the same in both lattices assuming that this already provides suffcient correction of b_4 and b_5 errors. Similarly to the sextupole spool pieces, all b_4 correctors and b_5 correctors in one arc belong to the same family. Misalignments are not taken into account. The minimum DA for both lattices at the three injection energies is presented in Table 4. As the results of

Table 4: Minimum Dynamic Aperture for Both HE-LHC lattices at Injection Energy

		450GeV	900GeV	1300GeV
without	18 cell	$58\,\sigma$	$97\,\sigma$	$123\,\sigma$
Errors	23 cell	$42\,\sigma$	$61\,\sigma$	$75\,\sigma$
all errors +	18 cell	$1.7\,\sigma$	$3.1\,\sigma$	$4.8\,\sigma$
b_3, b_4, and b_5	23 cell	$2.8\,\sigma$	$1.0\,\sigma$	$11.9\,\sigma$
correction				
b_3 errors only	18 cell	$2.2\,\sigma$	$4.5\,\sigma$	$7.4\,\sigma$
+ correction	23 cell	$3.3\,\sigma$	$7.5\,\sigma$	$12.6\,\sigma$
b_5 errors only	18 cell	$8.0\,\sigma$	$11.3\,\sigma$	$18.4\,\sigma$
+ correction	23 cell	$11.8\,\sigma$	$20.5\,\sigma$	$32.3\,\sigma$

the tracking studies especially at lower injection energies are below the target of $12\,\sigma$ increasing the number of correctors and also a higher number of corrector families is currently under study as a way to achieve sufficient DA.

CONCLUSION

Two possible lattice solutions for the HE-LHC have been presented. The LHC-like lattice provides a reasonable physical aperture at the lowest considered injection energy, but is limited in the energy reach. The second lattice on the other hand does allow to reach the targeted 27 TeV, however the aperture at 450 GeV appears challenging for collimation. The impact of magnetic field errors for both lattices at injection energy has been evaluated. With current correction scheme the minimum DA only in the case of the 23 cell lattice at the highest injection energy is close to the target value of $12\,\sigma$ of the LHC [1]. Future studies will focus on the correction of the non-linear errors at the lower injection energies to reach the target dynamic aperture.

REFERENCES

[1] O. Brüning *et al.*, "LHC Design Report", CERN, Geneva, Switzerland, CERN-2004-003, 2004.

[2] E. Metral *et al.*, "Update of the HL-LHC Operational scenarios for proton operation", CERN, Geneva, Switzerland, CERN-ACC-2018-002, 2018.

[3] F. Zimmermann *et al.*, "High-Energy LHC Design", presented at the IPAC'18, Vancouver, Canada, April-May 2018, paper MOMPF064, this conference.

[4] Y. Nosochkov *et al.*, "Optimized Arc Optics for the HE-LHC", presented at the IPAC'18, Vancouver, Canada, April-May 2018, paper MOMPF067, this conference.

[5] MAD-X, `http://madx.web.cern.ch/madx/`

[6] R. Bruce *et al.*, "Parameters for aperture calculations at injection for HL-LHC", CERN, Geneva, Switzerland, CERN-ACC-2016-0328, February 2016.

[7] I. Bellafont and R. Kersevan, "Studies on the beam induced effects in the FCC-hh", presented at the EuroCirCol Meeting, October 9th 2017

[8] R. Bruce, private communication, March 2018.

[9] L. van Riesen-Haupt *et al.*, "Experimental Interaction Regions for the High Energy LHC", presented at the IPAC'18, Vancouver, Canada, April-May 2018, paper MOPMK004, this conference.

[10] P. Mirave *et al.*, "Optics for RF Acceleration Section in IR4 for the High Energy LHC", presented at the IPAC'18, Vancouver, Canada, April-May 2018, paper MOPMK001, this conference.

[11] Sixtrack, `http://sixtrack.web.cern.ch/SixTrack/`

[12] S. Fartoukh and O. Bruning, "Field Quality Specifications for the LHC Main Dipole Magnets", CERN, Geneva, Switzerland, LHC Project Report 501, October 2001.

[13] M. Hofer, "Correction Circuits and Dynamic Aperture", presented at the FCC Week 2018, Amsterdam, April 2018.